Band-Gap Engineering of Semiconductor Nanowires through Composition Modulation

Yongqi Liang, Lin Zhai, Xinsheng Zhao, and Dongsheng Xu*

State Key Laboratory for Structural Chemistry of Unstable and Stable Species, College of Chemistry and Molecular Engineering, Peking University, Beijing 100871, People's Republic of China

Received: September 30, 2004; In Final Form: January 11, 2005

Alloyed ternary $CdS_{1-x}Se_x$ nanowires were synthesized by template-assisted electrodeposition, in which the ratio of S to Se in the nanowires was controlled by adjusting the relative amounts of the starting materials. Higher-resolution transmission electron microscopy (HRTEM) and X-ray diffraction (XRD) showed that the alloyed ternary $CdS_{1-x}Se_x$ nanowires are highly crystalline, and no phase-separated Cd was observed in these nanowires. Optical measurements indicated that the band-gap engineering can be realized in these $CdS_{1-x}Se_x$ nanowires through modulating the composition of S and Se. With broadly tunable optical and electrical properties, these alloyed nanowires could be used in color-tuned nanolasers, biological labels, and nanoelectronics.

Introduction

The success of compound semiconductors in optoelectronics and integrated circuits is largely attributed to the capability of energy-band engineering through composition modulation. Composition modulated II-VI and III-V based semiconductors are now widely used to fabricate the superlattices and heterojunction bipolar transistors (HBTs) with a two-dimensional film configuration.[1] Nanowires are an important class of material potentially useful as a key building block in "bottom-up" manufacturing nanotechnology.[2] Similar to the ideas in the two-dimensional counterpart, designed energy-band engineering of nanowires is expected to yield nanoscale devices with interesting properties and functions. In the past few years, extensive attention has been devoted to tune the band gap of the nanowires through the quantum confinement effect.[3,4] However, progress in this field only gives the ability to generate nanowires with diameters in a limited range, in which the quantum confinement effect is not prominent. On the other hand, the diameter tuning of electronic, optical, and magnetic properties may cause problems in many applications. For example, the formation of the intrinsic Fabry−Perot cavity for nanolaser of individual nanowires requires its diameter to be larger than a critical value.[5,6] In this paper, we present a class of alloyed II-VI semiconductor ternary $CdS_{1-x}Se_x$ nanowires with continuous tuning of the band gap through composition modulation. The alloyed nanowires of ternary $CdS_{1-x}Se_x$ were prepared by a template-assisted electrodepsoition process.[7,8] The ratio of S to Se in the nanowires was controlled by adjusting the relative amounts of the starting materials. Optical measurements indicate that the band gaps of these well-structured nanowires are continuously tuned from 1.75 eV (CdSe) to 2.44 eV (CdS).

Experimental Section

$CdS_{1-x}Se_x$ nanowires were galvanostatically electrodeposited into the pores of anodic aluminum oxide (AAO) membranes (20 nm in diameter) from dimethyl sulfoxide (DMSO) containing 0.05 M $CdCl_2$, element S, and Se at 160 °C. Before electrodepositon, a conductive Au layer was thermally evaporated on one side of the AAO template. A typical series of the starting materials with molar ratios Se to (Se + S) in the solutions varied as 0.47, 0.40, 0.34, 0.25, 0.14, and 0.08 were used to obtain different x for $CdS_{1-x}Se_x$ nanowires. For example, in the preparation of a bath with a Se/(S + Se) molar ratio of 0.25, 0.2275 g of $CdCl_2 \cdot 2.5H_2O$ (>99.0%), 0.0120 g of S (99.0%), and 0.0100 g of Se (>99.9%) were dissolved in 20.0 mL of DMSO (>99%) at 180 °C first and then cooled to 160 °C. The deposition current density was kept constant at 2.4 mA/cm^2, and the deposition time was 15 min. After electrodeposition, the nanowires embedded in the AAO template were then annealed at 400 °C under a N_2 atmosphere for 8 h. For ultraviolet−visible (UV−vis) absorption (Varian Cary 1E) and X-ray diffraction (XRD, Shimadzu 6000) characterization, the back Au layer of the nanowire/AAO/Au samples was removed by chemically dissolving them in 1.0 M NaCN aqueous solution. For scanning electron microscopy (SEM, FEI DB232), Raman, and photoluminescence (PL) characterization (Renishaw 1000 spectrometer), the AAO of the nanowire/AAO/Au was dissolved in 2.0 M NaOH solution for 4 h, and then, a supercritical drying process was used to avoid significant collapse to obtain the vertically aligned nanowire arrays on the Au substrates.[9] The composition determination of the alloyed ternary nanowires was carried out on an energy-dispersive X-ray (EDX, Oxford 6854) spectrometer attached to the scanning electron microscope. For transmission electron microscopy (TEM, JEOL CX200) and higher-resolution transmission electron microscopy (HRTEM, FEI Tecnai F30) analysis, the nanowires were detached from the Au substrate by immersion in an ethanolic supersonic bath for a few seconds, and then, one drop of the nanowire suspension was collected with a copper grid.

Results and Discussion

Figure 1a shows a typical SEM image of the $CdS_{1-x}Se_x$ nanowire sample on the Au substrates. It can be seen that large-area vertically aligned nanowire arrays are formed. These nanowires are uniform in lengths of 10 μm. The EDX spectrum (Figure 1b) taken from the same sample shows that the nanowires are composed of Cd, S, and Se, with an atom ratio of 0.97:0.75:0.25. The HRTEM image of an individual nanowire

* Corresponding author. E-mail: dsxu@pku.edu.cn.

10.1021/jp045566e CCC: $30.25
Published on Web 03/24/2005

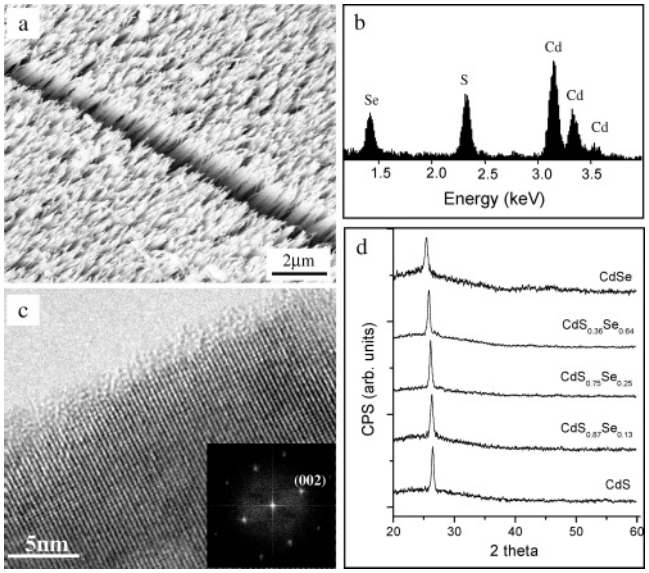

Figure 1. SEM image (a) and EDX spectrum (b) of the $CdS_{1-x}Se_x$ nanowire arrays by template-assisted electrodeposition. (c) High-resolution TEM image of an individual 20 nm $CdS_{1-x}Se_x$ nanowire. The inset in Figure 1c shows the corresponding Fourier transformation of the entire HRTEM image. (d) X-ray diffraction patterns of a series of $CdS_{1-x}Se_x$ nanowires embedded in the AAO templates.

(Figure 1c) displays a single crystalline wurtzite structure. The corresponding Fourier transformation of this HRTEM image (the inset in Figure 1c) indicates [001] as the growth direction for the $CdS_{1-x}Se_x$ nanowire. Furthermore, the similar single crystalline structures were also shown in the $CdS_{1-x}Se_x$ nanowires with different x values, which the interplanar spacing related to the {001} plane enhances with an increase of the Se concentrations in the nanowires. The single crystalline nature of these nanowires implies a well-structured alloying process during electrodeposition.

The overall crystallinity of the nanowire arrays is examined by XRD patterns, as shown in Figure 1d. It is found that the (002) peak of wurtzite $CdS_{1-x}Se_x$ is dominant, and usually, it is the only peak in the spectrum. This confirms that the *c*-axis of hexagonal crystal is preferentially aligned along the direction normal to the substrates. No phase-separated Cd is observed in these nanowire samples. In addition, $CdS_{1-x}Se_x$ is safely assumed to belong to the same group as CdS and CdSe with lattice parameters modulated between CdS ($a = 4.140$ Å, $c = 6.719$ Å; JCPDS 41-1049) and CdSe ($a = 4.299$ Å, $c = 7.010$ Å; JCPDS 08-459). As a result, the positions of the (002) peak in XRD patterns shift from 26.5° to 26.3, 26.1, 25.8, and 25.4° as the concentration of Se (x) in $CdS_{1-x}Se_x$ increases from 0 to 0.13, 0.25, 0.64, and 1.00, respectively.

Figure 2a shows the micro-Raman spectra of a series of the $CdS_{1-x}Se_x$ nanowire samples at room temperature. Determined by the mass of the constituent atoms and their respective bonding force constants, $CdS_{1-x}Se_x$ is classified in the "two-mode-behavior" alloys.[10] In these samples, peaks of ~200 cm^{-1} are assigned to a CdSe-like longitudinal optical mode (LO_1), while peaks of ~300 cm^{-1} are attributed to a CdS-like longitudinal optical mode (LO_2). It can be found that, as the x value in $CdS_{1-x}Se_x$ nanowires varies from 0 to 1, LO_1 and LO_2 would shift to 203 and 208 cm^{-1} from 195 and 301 cm^{-1}, respectively. Meanwhile, the overtones of LO_1 and LO_2 are also well assigned in all of these spectra. The difference between the frequencies of LO_2 and LO_1 (Figure 2b) showed a linear dependence on the composition of the bulk $CdS_{1-x}Se_x$, $LO_2 - LO_1$ (cm^{-1}) = $110 - 42x$, which is well coincident with the literature.[11] The $LO_1 + LO_2$ modes that appear in the ternary samples also indicate that well-structured ternary $CdS_{1-x}Se_x$ alloys are formed in the nanowires.

To understand the relationship between the band gap and the composition in these nanowires, we measured the UV−vis absorption spectra of a set of $CdS_{1-x}Se_x$ nanowire samples. In Figure 3, we can clearly see that the absorption edge blue shifts with a decrease of the Se ratio in the ternary nanowires. The widely used method of plotting $(\alpha h\nu)^2$ versus the energy $h\nu$ is adopted to determine the band gap of the nanowires.[12] The band-gap values of the $CdS_{1-x}Se_x$ nanowires deduced from the absorption curves are 1.75, 1.88, 1.98, 2.19, 2.33, and 2.44 eV, with the x value in a sequence of 1.00, 0.72, 0.51, 0.26, 0.11, and 0.

Figure 4a shows the PL spectra of the CdS nanowires. The peak located at ~2.43 eV corresponds to the band-gap transition of CdS, and an intense broad peak at ~1.62 eV is attributed to the anionic antisite S_{Cd} defects that might exist in the nanowires.[13,14] As an excitation energy of 488 nm is in resonant condition with the band gap of the nanowires, a resonant Raman

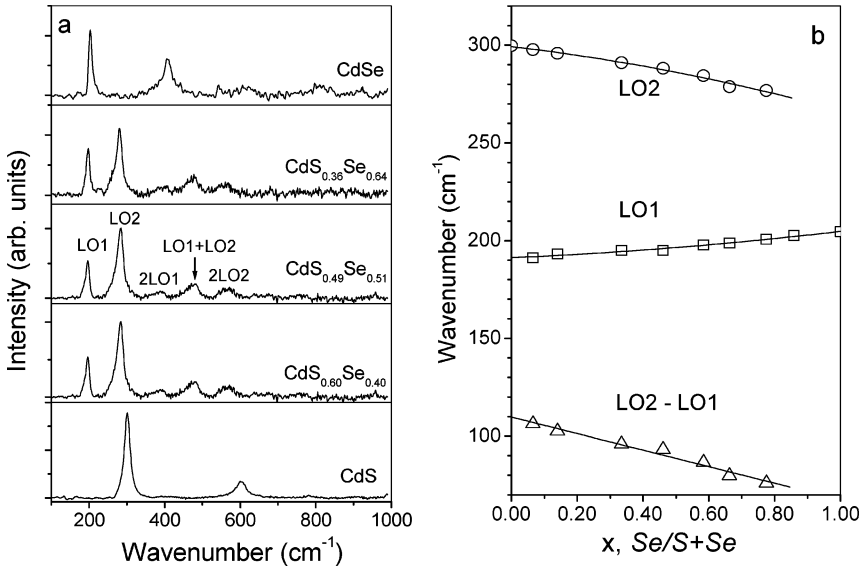

Figure 2. (a) Microscopic Raman spectra of a set of $CdS_{1-x}Se_x$ nanowire samples. The accuracy of the measurement is 1 cm^{-1}. The spectra are pixel-by-pixel background subtracted. (b) Variation of longitudinal optical model in Figure 2a with the composition in $CdS_{1-x}Se_x$ nanowires.

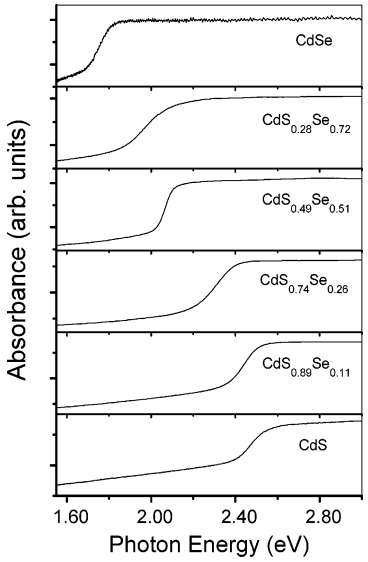

Figure 3. UV−vis absorption spectra of a series of $CdS_{1-x}Se_x$ nanowires embedded in the AAO membranes.

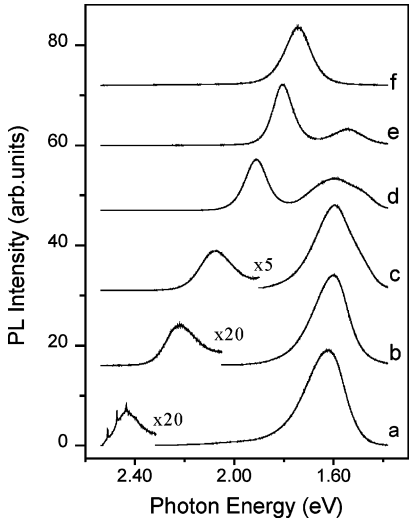

Figure 4. PL spectra of a series of $CdS_{1-x}Se_x$ nanowires with different x values: (a) 0; (b) 0.22; (c) 0.40; (d) 0.64; (e) 0.87; (f) 1.00. All the samples were excited with a 488 nm Ar^+ laser at room temperature.

signal superimposed on the fluorescent signal is also observed. Figure 4b−e displays the PL spectra from a series of ternary $CdS_{1-x}Se_x$ nanowires. It is found that the peak maximum position related to the band-gap transition continuously red shifts with an increase of the x value in the $CdS_{1-x}Se_x$ nanowires. The typical full width at half-maximum (fwhm) of the band-edge PL for these nanowires is ∼35 nm, which is comparable to those of the widely used II-VI spherical quantum dots.[15,16] Such narrow peaks of the band-edge fluorescent emission also imply that the distribution of the composition in these $CdS_{1-x}Se_x$ nanowires is quite uniform. Meanwhile, we also found that, with enhancement of the Se ratio in the $CdS_{1-x}Se_x$ nanowires, the PL intensity of the band-gap transition increases, in contrast to the decrease of the PL intensity originating from the anionic antisite defects. As shown in Figure 4f, only a dominant peak at ∼1.74 eV was observed in pure CdSe nanowires. In addition, the PL quantum efficiency of these nanowires was estimated by comparing the integrated PL intensities of $CdS_{1-x}Se_x$ nanowires with an organic dye (rhodamine B with an absolute quantum yield of 50%) under the same settings,[17] as shown in Table 1. In the literature, the typical PL quantum yields for the

TABLE 1: PL Quantum Yields of the $CdS_{1-x}Se_x$ Nanowires with Different x Values[a]

	x					
quantum yield	0.00	0.22	0.40	0.64	0.87	1.00
overall emission	8%	7.5%	7%	5%	4%	3%
band-edge emission	0.05%	0.05%	0.3%	1.7%	2%	3%

[a] Rhodamine B with an absolute quantum yield of 50% was used as a reference for comparison. All the samples were excited by an Ar^+ laser (488 nm) at room temperature.

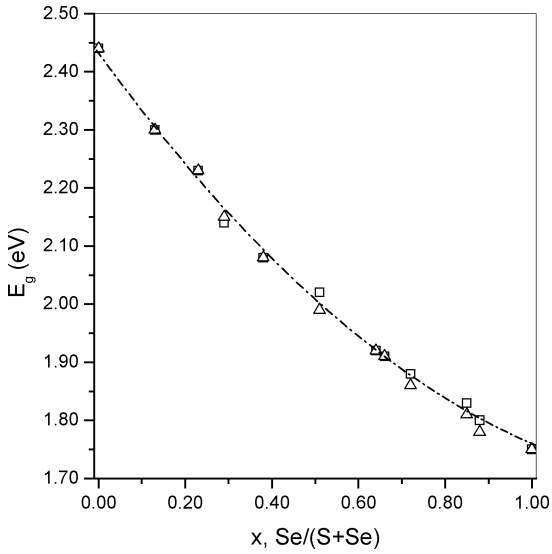

Figure 5. Band gaps (E_g) of the $CdS_{1-x}Se_x$ nanowires versus the concentration ratio of Se/(Se + S): (□) E_g (PL); (Δ) E_g (absorption). The dashed line is a polynomial fitted curve for the E_g of the $CdS_{1-x}Se_x$ nanowires determined by PL spectra.

as-prepared CdS and CdSe nanocrystals at room temperature were around 10%.[16]

Furthermore, the band gap of the $CdS_{1-x}Se_x$ nanowires, deduced from the optical absorption spectra and the PL spectra, is plotted versus the concentration ratio of Se/(Se + S) in Figure 5. We found that the variation of the band gap with concentration deviates from linearity, which is in agreement with the previous observation on CdS:Se single crystal.[18] The composition variations of the band gap can be fitted to a relationship described as follows:

$$E_g(x) = E_g(0) - \alpha x + \beta x^2$$

where x is the concentration ratio of Se to (Se + S), $E_g(0)$ is the band gap of pure CdS nanowires, and α and β are constants. For the data deduced from the optical absorption spectra, the estimated values of $E_g(0)$, α, and β were 2.44, 1.06, and 0.38 eV, respectively. The corresponding values for the data from the PL spectra were 2.43, 1.03, and 0.36 eV, respectively.

Very recently, composition modulation was applied to the preparation of nanowires for $Bi_{2-x}Sb_xTe_3$, $Bi_2Te_{3-y}Se_y$,[19] $GaAs_{0.6}P_{0.4}$, $InAs_{0.5}P_{0.5}$,[20] and $Ag_2Se_{1-x}Te_x$,[21] but less attention has been put on the energy band engineering in nanowires through this concept. Routkecitch et al. claimed that they obtained $CdS_{1-x}Se_x$ and $Zn_{1-x}Cd_xS$ nanowires and provided UV absorption spectra of the nanowires. However, the higher potentials they used in the ac deposition cycle (>5 V) could result in the co-deposition of Cd and their XRD spectra revealed significant phase-separated Cd in those nanowires.[7] In addition, for the ac process, the rate and direction of the diffusion would vary with the alternation of the electric field and thus make a

high density of defects and small polycrystalline structure in the nanowires.[7,22] Under dc deposition conditions, it is easy to control the potential as being no more than the co-deposition potential of Cd, and the diffusing process reaches a steady state. Thus, the defects in the electrodeposited nanowires are largely decreased. Both the electron microscopy and fluorescent emission in our results demonstrate that the alloyed ternary $CdS_{1-x}Se_x$ nanowires are highly crystalline, and also, the XRD pattern obviates the possibility of phase-separated Cd in the nanowires. Of the most importance, we show that the band-gap engineering can be realized in the highly crystalline $CdS_{1-x}Se_x$ nanowires through modulating the composition of S and Se.

Conclusion

In summary, we have achieved continuous band-gap tuning through composition modulation in highly crystalline $CdS_{1-x}Se_x$ nanowires synthesized by AAO template-assisted electrodeposition. This may open the possibilities of developing a variety of ternary or quaternary semiconductor nanowires based on II-IV and III-V materials.[8,20] With broadly tunable optical (fluorescent emission and refractivity) and electrical (carrier mobility and voltage threshold) properties, these alloyed nanowires can be used in color-tuned nanolasers, biological labels, and nanoelectronics.

Acknowledgment. We thank J. P. Zhang and X. C. Ai at the Institute of Chemistry, Chinese Academy of Science, for helpful discussions. This work is supported by the Major State Basic Research Development Program (Grant No. 2000077503, G1999075305) from the Ministry of Science and Technology, China, and the NSFC (Grant No. 20433010, 20333010).

References and Notes

(1) Kroemer, H. *ChemPhysChem* **2001**, *2*, 490.

(2) Xia, Y.; Yang, P.; Sun, Y.; Wu, Y.; Mayers, B.; Gates, B.; Yin Y.; Kim, F.; Yan, Y. *Adv. Mater.* **2003**, *15*, 353.

(3) (a) Gudiksen, M. S.; Lieber, C. M. *J. Am. Chem. Soc*. **2000**, *122*, 8801. (b) Gudiksen, M. S.; Wang, J.; Lieber, C. M. *J. Phys. Chem. B* **2002**, *106*, 4036.

(4) Ma, D. D. D.; Lee, C. S.; Au, F. C. K.; Tong, S. Y.; Lee, S. T. *Science* **2003**, *299*, 1874.

(5) (a) Huang, M. H.; Mao, S.; Feick, H.; Yan, H.; Wu, Y.; Kind, H.; Weber, E.; Russo, R.; Yang, P. *Science* **2001**, *292*, 1897. (b) Choi, H. J.; Johnson, J. C.; He, R.; Lee, S. K.; Kim, F.; Pauzauskie, P.; Goldberger J.; Saykally, R. J.; Yang, P. *J. Phys. Chem. B* **2003**, *107*, 8721.

(6) Duan, X.; Huang, Y.; Agarwal, R.; Lieber, C. M. *Nature* **2003**, *421*, 241.

(7) Routkecitch, D.; Tager, A. A.; Haruyama, J.; Almawlawi, D.; Moskovits, M.; Xu, J, M. *IEEE Trans. Electron. Devices* **1996**, *43*, 1646.

(8) (a) Xu, D.; Xu, Y.; Chen, D.; Guo, G.; Gui, L.; Tang, Y. *Adv. Mater.* **2000**, *12*, 520. (b) Xu, D.; Shi, X.; Guo, G.; Gui, L.; Tang, Y. *J. Phys. Chem. B* **2000**, *104*, 5061. (c) Xu, D.; Xu, Y.; Chen, D.; Guo, G.; Gui, L.; Tang, Y. *Chem. Phys. Lett*. **2000**, *325*, 340.

(9) The supercritical drying was carried out in a 0.5 L autoclave. The nanowire samples without AAO were transferred to the autoclave filled with ethanol. The ethanol in the pores was replaced by liquid CO_2 (T_c = 31.1 °C and P_c = 73.8 bar) by flushing at a speed of 4−6 cm^3/min at 16 °C and 58 bar. After the autoclave was filled with liquid CO_2 and the residual ethanol was at or below the 10 ppm level, the temperature of the autoclave was raised to 44 °C in 2 h, reaching a pressure of ∼100 bar. Finally, CO_2 underwent a transformation from the supercritical phase to the gas phase by decreasing the pressure while keeping the temperature at 44 °C.

(10) Pagliara, S.; Sangaletti, L.; Depero, L. E.; Capozzi, V, Perna, G. *Solid. State Commun*. **2000**, *116*, 115.

(11) Miyoshi, T.; Nakatsuka, R.; Matsuo, N. *Jpn. J. Appl. Phys., Part 1* **1995**, *34*, 1835.

(12) Pankove J. I. *Optical properties in semiconductors*; Prentice Hall: Engelewood Cliffs, NJ, 1971.

(13) Perna. G.; Ambrico. M.; Capozzi. V.; Smaldone. D.; Martino. R. *J. Lumin*. **1997**, *72*−*74*, 90.

(14) Pan, J. L.; Mcmanis. J. E.; Osadchy. T.; Grober. L.; Woodalll. J. M.; Kindlmann. P. J. *Nat. Mater*. **2003**, *2*, 375.

(15) Qu. L. H.; Peng. X. G. *J. Am. Chem. Soc*. **2002**, *124*, 2049.

(16) Murray, C. B.; Norris, D. J.; Bawendi, M. G. *J. Am. Chem. Soc*. **1993**, *115*, 8706.

(17) Bailey, R. E.; Nie, S. *J. Am. Chem. Soc*. **2003**, *125*, 7100.

(18) Pedrotti, F. L.; Reynolds, D. C. *Phys. Rev.* **1962**, *127*, 1584.

(19) (a) Martin-Gonzalez. M.; Prieto, A. L.; Gronsky, R.; Sands, T.; Stacy, A. M. *Adv. Mater*. **2003**, *15*, 1003. (b) Martin- Gonzalez. M.; Snyder, G. J.; Prieto, A. L.; Gronsky, R.; Sands, T.; Stacy, A. M. *Nano Lett*. **2003**, *3*, 973.

(20) Duan, X.; Lieber, C. M. *Adv. Mater*. **2000**, *12*, 298.

(21) Chen, R.; Xu, D.; Guo, G.; Gui, L. *Electrochem. Commun*. **2003**, *5*, 579.

(22) Hutchison, J. L.; Routkevitch, D.; Moskovits, M.; Nayak, R. R. *Inst. Phys. Conf. Ser*. **1997**, *157*, 389.